L-H Threshold Studies in NSTX

S.M. Kaye 1), R. Maingi 2), D. Battaglia 2), R. E. Bell 1), C.S. Chang 3), B.P. LeBlanc1), J. Hosea 1), H. Kugel 1), H. Meyer 4), G.-Y. Park 3), J.R. Wilson 1)

[1] Princeton Plasma Physics Laboratory, Princeton University, Princeton, NJ 08543
[2] Oak Ridge National Laboratory, Oak Ridge, TN 37831
[3] New York University, New York, NY
[4] UKAEA Fusion, Culham, UK

email contact of main author: skaye@pppl.gov

Abstract. Recent experiments in the low aspect ratio National Spherical Torus Experiment (NSTX) have been run in support of the high priority ITER and ITPA issue of access to the H-mode. Specifically, a series of L-H threshold experiments have addressed the effect of plasma ion species, applied 3D fields, wall conditioning, plasma current and plasma shape/X-point position on the L-H power threshold and local parameters leading up to the transition. Experiments have indicated lower threshold power for deuterium vs helium plasmas, discharges with no applied edge fields, with lithium conditioning, with lower triangularity, and with lower plasma current. The latter two observations are consistent with XGC0 calculations showing a deeper E_r well and stronger E_r shear near the edge at lower triangularity or at lower current. To within the constraints of temporal and spatial resolutions, no systematic difference in T_e, n_e, p_e, T_i, v_ϕ or their derivatives was found in discharges that transitioned into the H-mode versus those at slightly lower power that did not. Finally, it was found that RF-heated discharges attained values of $H_{98y,2}$~1 in ELM-free conditions for powers just above the power threshold. NBI heated, ELM-free H-modes could also achieve $H_{98y,2}$~1, but only after ~50 ms after the transition.

1. Introduction

Attempts to characterize and understand the physics of the L-mode to H-mode transition have been at the forefront of tokamak physics studies since the H-mode was discovered in 1982 [1,2]. Initial experimental studies focused on global parametric dependences or the heating power required for transition into the H-mode, such as those on density, plasma current, toroidal field and plasma size in conventional aspect ratio tokamaks. These studies led to the development of parametric scalings in support of the development of the ITER physics basis [3,4]. These experimental studies indicated a large range of heating power even for similar global discharge parameters, thus indicating the importance of other, as yet unquantified parameters. Experimental studies extended into low aspect ratio [5] and examining the role of edge parameters and their gradients [6], but results across machines were not universal. Theory also attempted to explain the L-H transition [7 and references therein], but no single theory emerged. It is generally believed that edge ExB shear, through mean or zonal flows, is important in turbulence suppression that can lead to the L-H transition [7 and references therein], but this has not been yet proven convincingly.

Knowing the characteristics, and more importantly the underlying physics, of the L-H transition has been identified by the ITER Physics group as a high priority issue. Operation in the H-mode is critical to the success of ITER, and knowledge of the transition characteristics beyond what is already known was requested in order to be able to refine the expectations for ITER with more precision. In this work, we report results of dedicated experiments carried out in the The National Spherical Torus Experiment (NSTX) in support of the high priority ITER and ITPA needs, addressing such issues as effect of plasma ion species, applied 3D fields, wall conditioning, plasma current and plasma shape/X-point position on the L-H power threshold (P_{LH}) and local parameters leading up to the transition. NSTX is a low aspect ratio tokamak with R/a=0.85/0.65 m ~1.3, which operates with neutral beam and High Harmonic

Fast Wave (HHFW) heating powers up to 7 MW and 4 MW respectively. NSTX typically operates at toroidal fields of B_T up to 0.55 T, plasma currents I_p of up to 1.4 MA, with elongations κ up to 3 and triangularity δ up to 0.8. NSTX has implemented an external coil set capable of applying n=1 to 3 fields at the plasma edge, and it also has conditioned the plasma facing graphite tiles with evaporated lithium.

2. L-H Power Threshold Dependences

Since initial ITER operations will be with either hydrogen or helium plasmas, it is important to understand how the L-H power threshold scales with working gas. Initial studies on this were performed in ASDEX-Upgrade, using ECH heating in pure deuterium and helium plasmas [8]. The results of these experiments showed no difference in power threshold for the two plasma species; furthermore, the density for which the power threshold is a minimum was also found to be similar for the two species. Dedicated experiments were performed in NSTX to follow up on this initial work. The NSTX experiments utilized High Harmonic Fast Wave Heating (HHFW), which allowed the studies to be performed also in pure deuterium and pure helium plasmas. Furthermore, the HHFW, with a wavenumber of k_θ=-8 m^{-1}, was injected with a power waveform that increased up to 3.5 MW power at the antenna, flattoped at that value for approximately 60 ms, then decreased. This power waveform allowed a precise determination of both the L-H and H-L transitions. An example of a deuterium discharge is shown in Fig. 1. The L-H transition occurred at the peak power, as indicated by the drop in the D_α and the increase in line-integral density. In this particular discharge, no H-L back transition was evident. In helium discharges, the L-H transition could not be determined by the D_α drop; instead, careful analysis of the change in edge density profile was used to determine both the forward and backward transition. An example of this is shown for a helium plasma in Fig. 2. The transitions can be seen by the increase (or decrease) in the gradients of both T_e and n_e at the plasma edge.

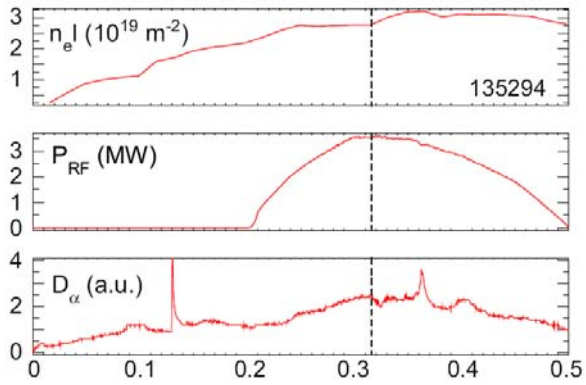

Fig. 1 Line integral density, HHFW power waveform and D_a emissivity for a D^+ discharge.

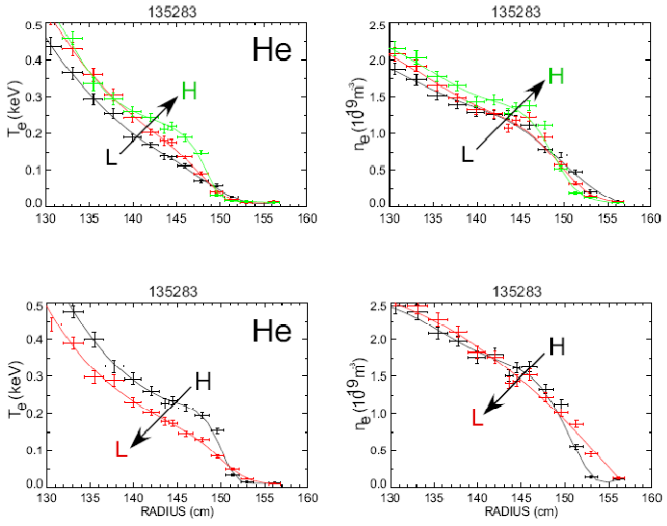

Fig. 2 Temperature and density profiles near the plasma edge spanning the L-H (top) and H-L (bottom) transitions for a helium discharge.

To determine L-H and H-L transition powers, the actual HHFW power heating the plasma had to be determined. To do this, a perturbation method was used which took advantage of occasional dropouts of the HHFW power. From the rate of change of plasma stored energy and the ultimate level of energy to which

the plasma relaxed after the power dropout, this actual heating power could be estimated. For the range of discharges, the average efficiency, defined as the ratio of the calculated heating power to power at the antenna, was approximately 0.30±0.11, with slightly higher efficiencies for helium (0.33) than for deuterium (0.28). The threshold power was defined as this heating power plus the ohmic power less the time rate of change of stored energy at the time of the transition. The set of discharges used to study the threshold powers exhibited a small range of densities, with the line-averaged density varying from 1.8 to 2.2 x 10^{19} m^{-3} at the time of the L-H transition (most of the discharges were within a 15% range). Analysis showed that, within this small range, the power threshold scaled almost linearly with density, and was not inconsistent with the $n_e^{0.75}$ dependence seen in various L-H power threshold scalings. In this work, the threshold power is normalized by the line-averaged density ($n_e^{1.0}$).

The results of this isotope scan are shown in Fig. 3, where the power threshold is plotted vs discharge number, and which indicates that the L-H power threshold is approximately 20-40% greater in helium than in deuterium. The error bars reflect the uncertainty primarily in the determination of the heating efficiency overall, as well as for the differences in efficiency between deuterium and helium (indicated by the two symbols for each discharge, one representing the average efficiency and the other representing the efficiency for that particular species). As can also be seen by the open symbols, the H-L transitions occurred essentially at the same power level as the L-H transitions, indicating little if any hysteresis within this parameter range. It is interesting to note that in NSTX, there would be no difference in threshold powers for helium and deuterium if the dW/dt term were omitted from the definition of P_{LH}, with the threshold power being merely the sum of the HHFW heating and ohmic powers. For this definition of threshold power, there is a clear indication of hysteresis, with the H-L transition occurring at significantly lower normalized power than the L-H transition. This means that once in the H-mode, the discharge is able to remain there even with heating powers, defined in this fashion, lower than that required for entry.

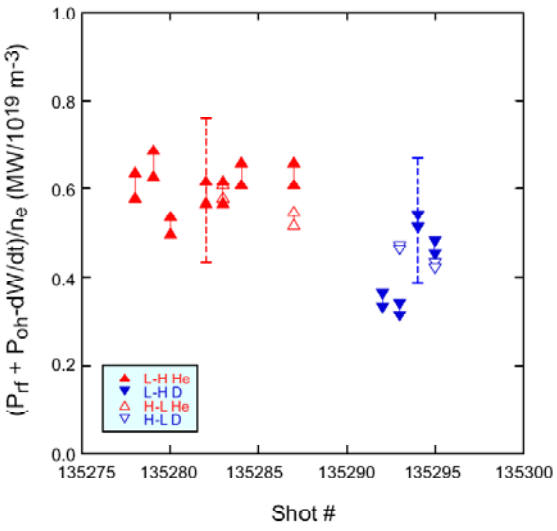

Fig. 3 Threshold power for L-H (solid) and H-L (open) helium (red) and deuterium (blue) HHFW discharges.

Another key dependence studied in NSTX was that on applied edge magnetic perturbations. NSTX is equipped with a set of external coils able to generate magnetic perturbations with toroidal mode numbers from 1 to 3, with field amplitudes of several Gauss at the plasma edge [9]. These coils have been used for error field correction, low-n edge mode control and controlled generation of ELMs. The importance of this study is related to the possible need for ELM control coils in ITER. Operating scenarios are envisioned in which the magnetic perturbations are applied prior to the L-H transition in order to suppress even the first ELM that might be driven unstable once the ITER plasma is in the H-mode. Thus, the question is what effect these applied fields might have on the power threshold. Dedicated experiments using n=3 applied fields were performed in NSTX, and the results are shown in Fig. 4. Neutral beams were used to heat the plasma in these discharges. The figure compares discharges in blue and red, for which n=3 fields were applied, with a baseline discharge in

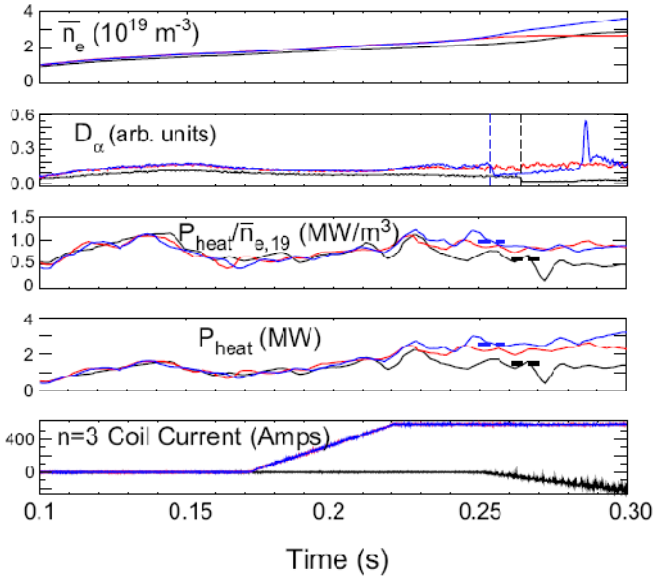

Fig. 4 Comparison of discharges showing the effect of applied 3D fields on the L-H threshold power.

black in which no n=3 field was applied (see n=3 coil current in bottom panel). The baseline discharge, without applied n=3 fields, showed a power threshold of approximately 1.4 MW (and power threshold normalized to plasma density of 0.55 MW/10^{19}m^3), as compared to the power threshold of 2.6 MW and normalized threshold of 1.0 MW/10^{19}m^3 (note that this power threshold is determined using the fact that the discharge in red remained in L-mode, while the one in blue, at slightly higher power, transitioned into the H-mode). Interestingly, comparison of toroidal and poloidal rotation velocities near the plasma edge showed no difference between the discharge without applied n=3 and those with applied n=3, indicating that the difference in power threshold is a magnetic configuration, rather than rotation shear, effect. Theoretical work is presently underway to help identify the difference among these discharges that could explain their different evolution.

A unique observation in NSTX is the dependence of power threshold on plasma current, a dependence that is not seen at higher aspect ratio. In neutral beam heated discharges at 0.7 MA, the L-H threshold power was determined to be 1.6 MW, or 0.7 MW/10^{19}m^3 when normalized to line averaged density. At 1.0 MA, the power threshold nearly doubled, increasing to 3.1 MW and 1.2 MW/10^{19}m^3 respectively. These results are consistent with earlier observations in ohmic plasmas in NSTX [9]. XGC0 [10] calculations were performed in an attempt to understand this current dependence. In XGC0, the radial electric field is calculated within the neoclassical framework using input data that includes the toroidal rotation and determination of the particle losses in the real magnetic geometry. The radial electric field for discharges that transition into the H-mode at the two current levels mentioned above are shown in Fig. 5. The times taken for the calculation are just prior to the L-H transition time. The lower current discharge clearly shows a deeper E_r well and stronger E_r shear than that at the higher current. E_r wells for both the higher and lower current cases are shallower for discharges that remained in the L-mode. The E_r well difference is caused by the difference in thermal ion loss cone near the plasma edge for the two different currents. For the lower current, the lower energy particles (up to 200 eV and with large $v_\parallel/v_\perp$) are preferentially lost relative to the higher current case, where the loss cone moves energies higher than the bulk of the ion population at that location.

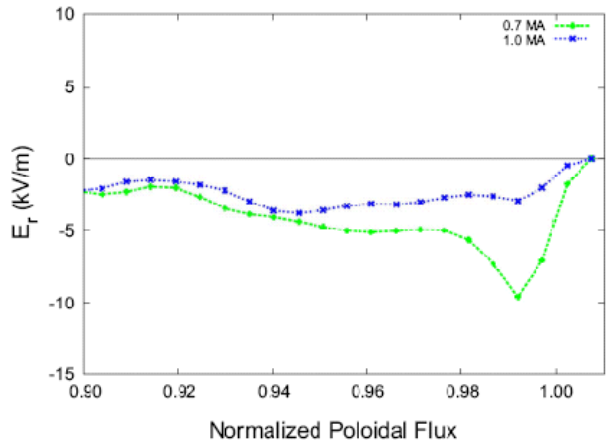

Fig. 5 Radial electric field computed from XGC0 for 0.7 MA (green) and 1.0 MA (blue) discharges.

The differences in the E_r wells leads to differences in the radial electric field shear, dE_r/dr, which are believed to be fundamental for the L-H transition. In the discharges studied above, the E_r shear for the lower current case is about a factor of two greater than that in the high current case for the discharges that transition into the H-mode (~8e6 vs ~4e6 V/m^2). On the other hand, the E_r shear values for those discharges that remained in the L-mode are both lower, although the lower current L-mode plasma still had an E_r shear value greater than that of the higher current L-mode (~4e6 vs ~1e6 V/m^2). Thus, it seems that for these discharges, ~4e6 V/m^2 appears to be the E_r shear threshold necessary for achieving H-mode.

The dependence of P_{LH} on plasma current in NSTX but not at higher aspect ratio can be understood qualitatively by noting that the fraction of trapped particles increases with decreasing aspect ratio. The width of the banana orbit of these particles is larger for particles with higher initial parallel velocity and for lower plasma current. In addition, the toroidal gyroradius of these trapped particles must also be taken into account, and NSTX operates at a toroidal magnetic field that is typically an order of magnitude less than that at higher aspect ratio. Given these features, the edge thermal ions in NSTX are more prone to loss than those at higher aspect ratio, and this may be why the sensitivity to plasma current is apparent at low aspect ratio.

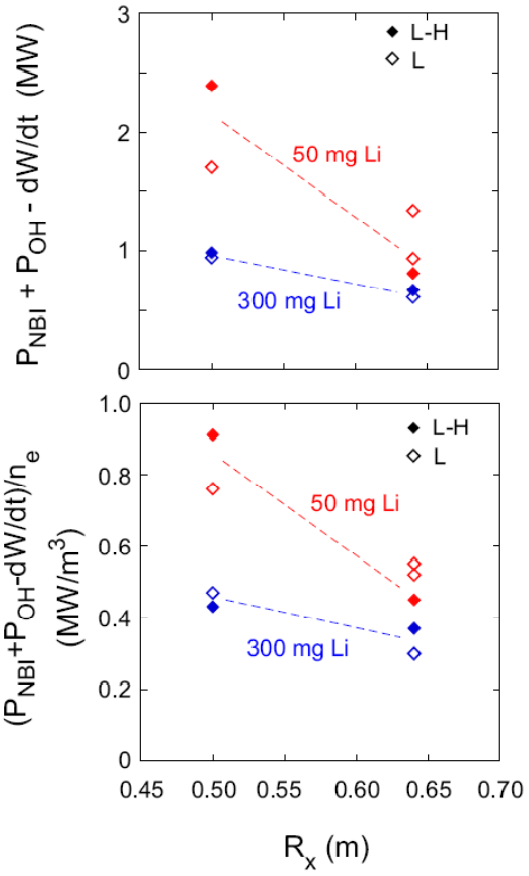

Fig. 6 L-H power threshold (top) and power threshold normalized by density (bottom) as a function of X-point radius for two different lithium evaporation rates. The stars are discharges that transitioned into the H-mode, while the squares are discharges that remained in L-mode.

Motivated by XGC0 calculations which show strongest ion loss and largest edge E_r and E_r' when the X-point is at large R, experiments assessing the L-H threshold power as a function of X-point radius, as reflected by differing triangularity were performed. Initial experiments exploring this dependence had mixed results due to secular variations in the magnitudes of P_{OH} and dW/dt as a function of triangularity [12]. A dedicated experiment was recently performed to examine the triangularity (X-point radius) dependence of the L-H threshold controlling the above parameters as much as possible. Shown in the Fig. 6 are the results of the experiment done at two different Lithium evaporation rates. Plotted are the powers (top panel) and density-normalized powers (bottom panel) as a function of X-point radius. The data clearly show a trend of lower threshold power at larger X-point radius (lower triangularity), consistent with the XGC0 results. The L-H threshold power is well determined in this experiment, as can be seen by the differences in power in data taken just before the L-H transition (solid diamonds) and those that remained in L-mode (open diamonds).

The last global dependence to discuss is that on wall conditioning. NSTX has been utilizing between-shots lithium evaporation on the graphite plasma facing components in an

attempt to reduce recycling and control particle density. Typically, between 50 and 100 mg of lithium is deposited between plasma discharges, and this has resulted in increased electron and energy confinement and a suppression of EL Ms in H-mode plasmas [13]. Use of lithium has led to a significant reduction in the L-H power threshold as well. A comparison of two similar discharges, but one with lithium conditioning and one without and after the lithium conditioning effects wore off, showed that without lithium, P_{LH}~2.7 MW, and with lithium, P_{LH}~1.4 MW. It should be noted that the discharge with lithium had significantly lower density, so a better comparison is with P_{LH}/n_e, and here the discharge without lithium had a threshold of 0.9 MW/10^{19}m^3, while the one with had a threshold of 0.55 MW/10^{19}m^3. This trend is supported by the difference in P_{LH} between discharges with high and low lithium evaporation rates shown in Fig. 6. Further analysis is underway to attempt to understand the cause of this difference, including the effect of differing neutral density on the threshold power [14].

3. Effect of Local Parameters on the L-H Transition

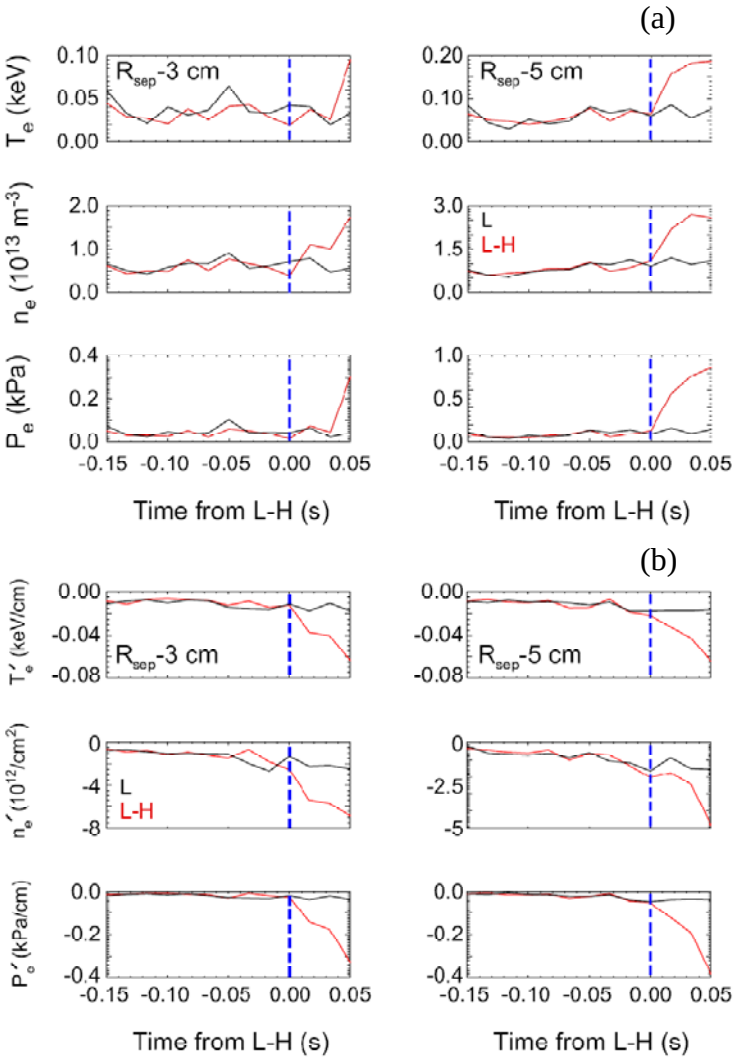

Fig. 7 T_e, n_e and p_e (top) and their gradients (bottom) evolution leading up to the L-H transition (t=0.0 s), shown for the discharge in red. The discharge in black remained in L-mode.

It is widely believed that the physics behind the L-H transition is tied more to local than to global processes. While the global heating power parameter may be a reasonable characterization for knowing approximately what is needed for H-mode access, there are effects that are not reflected and difficult to quantify using this global approach. Therefore, it has become more apparent that the study of how local edge parameters and their gradients change leading up to the L-H transition may yield insight into the underlying physics. The measurement of the local edge parameters in NSTX is, at this time, limited in terms of temporal and to some extent spatial resolution. The Thomson Scattering diagnostic (T_e, n_e) has a temporal/spatial resolution of 16 ms/1.5 cm, while the CHERS (T_i, v_ϕ, n_{carbon}) has 10 ms/2 cm resolution. Because of this, only the longer-time scale changes can presently be studied on NSTX; diagnosing changes on the time scale of ms or sub-ms is not possible.

A statistical study, using approximately twenty discharges was performed. The results shown in Fig. 7a and b is a comparison of two similar discharges, one that transitioned into the H-mode and one that did not, that reflect the overall conclusions from this statistical study. Plotted in Fig. 7a are the time traces of the electron temperature, density and pressure for a discharge that transitioned into the H-mode at t=0.0s on the abscissa (red) and one that did not (black). Traces are plotted at radial positions 3 and 5 cm inside the separatrix. As can be seen, no difference in these local quantities, to within the spatial and temporal resolution of the data, is seen for either radial position. Once in the H-mode, the discharge shown in red clearly shows an increase in these quantities, reflecting the buildup of the edge gradients, but this occurs after the transition. The gradients of these quantities at these two radial positions are shown in Fig. 7b, and again, to within the data resolution, no difference can be seen between the L and the L-H discharge prior to the transition.

4. Confinement Quality Following the L-H Transition

The initial ITER heating capabilities are expected to provide enough power for transition into the H-mode, although given the uncertainties in the power threshold, the power level may not exceed P_{LH} by very much. This raises two important issues. The first is whether, once the discharge transitions into the H-mode and density begins to rise, can the discharge remain in H-mode? The NSTX results reported in Section 3 indicate that, with the P_{LH} definition that includes, dW/dt, the H-L transition occurs at the same normalized power as the L-H transition, indicating potential difficulty in remaining in the H-mode at constant power but increased density. Without the dW/dt term, hysteresis exists, and the discharge is able to remain in the H-mode even below the nominal L-H threshold power.

The other issue has to do with the confinement quality at powers just above the L-H threshold. The confinement quality is typically $H_{98y,2}$~0.8 in discharges that exhibit Type III ELMs just above the power threshold. In NSTX, however, with the lithium conditioning, ELMs can be eliminated. In these HHFW and neutral beam heated plasmas, $H_{98y,2}$~1 confinement can be obtained just after the L-H transition, as shown in Fig. 8. This is most clearly seen in the HHFW heated discharges, where $H_{98y,2}$~1 is seen within 10 ms of the transition. For neutral beam heated discharges, the H-factors are lower at this time, but they increase to $H_{98y,2}$~1 and above within approximately 50 ms of the transition, as the density increases. The 50 ms represents approximately one τ_E or two fast ion slowing down times. The precise recipe for obtaining these high H-factors is not yet clear. The NSTX data do indicate that plasma shaping is extremely important; the H-factors are higher with higher elongation or triangularity (the two are inseparable in these NSTX experiments), plus, the discharge development after the transition plays an important role as well. Additional experiments are planned to identify the controlling factors.

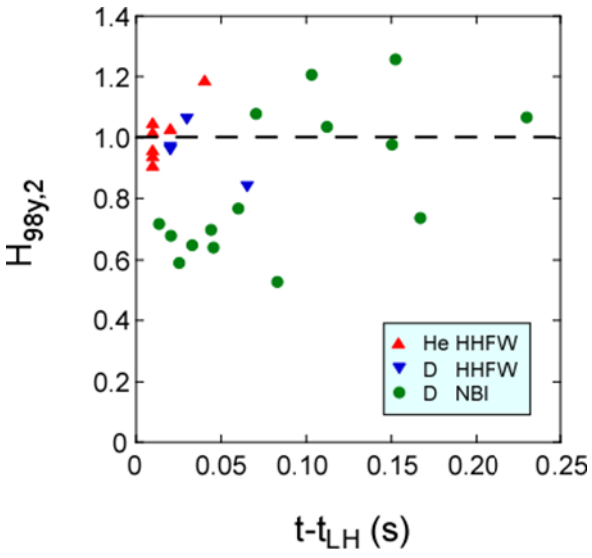

Fig. 8 Confinement quality for HHFW (red and blue) and NBI (green) discharges as a function of time from the L-H transition.

5. Summary

Dedicated NSTX experiments on the L-H power threshold have contributed to the ITER high priority physics requests on this topic. It was found that the L-H threshold power for helium was 20 to 40% greater than that for deuterium, and that is within the range of acceptability for ITER operation. It was also shown that wall conditioning using lithium can ease access to the H-mode significantly. On the other hand, there is a potential complication with utilizing an ELM suppression system which applies low-n magnetic perturbations to the plasma edge in a preventative mode prior to the transition, as this can result in at least a 50% increase in power threshold. Further, it appears that low triangularity plasmas are required for minimizing the power threshold. Unique to NSTX is the current dependence of the L-H threshold power; the sensitivity to this parameter in NSTX, and not at higher aspect ratio, is consistent with the higher trapping fraction and larger toroidal gyroradius at low aspect ratio. To within the spatial and temporal resolution of the relevant diagnostic systems on NSTX, no difference in edge parameters, or their gradients, was observed when comparing discharge periods leading up to the L-H transition, with those that remained in L-mode. Finally, $H_{98y,2}$~1 confinement quality could be obtained just after the L-H transition, although the precise recipe for obtaining this good confinement, including the discharge evolution, is still under study.

This work was supported by U.S. DOE Contract No. DE-AC02-09CH11466 (PPPL). The authors wish to thank P. Ryan and G. Taylor for their role in the HHFW-based experiments.

References

[1] Wagner, F., G. Becker, K. Behringer et al., Phys. Rev. Lett. **49** (1982) 1408.
[2] Kaye, S.M., M.G. Bell, K. Bol et al., J. Nucl. Mater. **121** (1984) 115.
[3] ITER Confinement Database and Modeling Group, "Threshold Power and Energy Confinement for ITER", in Proceedings of the 16th International Conference on Plasma Physics (Montreal, 1996) **2** (1997) 795.
[4] Martin, Y.R., T. Takizuka and ITPA CDBM H-mode Threshold Working Group, Journal of Physics:Conference Series **123** (2008) 012033.
[5] Kaye, S.M., M. Valovic, A. Chudnovskiy et al., Plasma Phys. Cont. Fusion **48** (2006) A429.
[6] Local variations
[7] Connor, J.W. and H.R. Wilson, Plasma Phys. Cont. Fusion **42** (2000) R1.
[8] Ryter, F., Putterich, T., Reich, M. et al., Nuc. Fusion **49** (2009) 062003.
[9] Coils
[10] Bush, C.E., M.G. Bell, R.E. Bell et al., Phys. Plasmas **10** (2003) 1755.
[11] Chang, C.S, S. Ku, and H. Weitzner, Phys. Plasmas **11**, (2004) 2649.
[12] Maingi, R., S.M. Kaye, R.E. Bell et al., Nuc. Fusion **50** (2010) 064010.
[13] Kugel, H.W., M.G. Bell, J.-W. Ahn, et al., Phys. Plasmas **15**, (2008) 056118.
[14] Lee, K.C., Phys. Plasmas **13** (2006) 062505.